Tetrahydrocannabinol (THC) Detection using Semiconductor-enriched Single-Walled Carbon Nanotube Chemiresistors

Sean I. Hwang,[a] Nicholas G. Franconi,[b] Michael A. Rothfuss,[b] Kara Bocan,[b] Long Bian,[a] David L. White,[a] Seth C. Burkert,[a] Raymond W. Euler,[a] Brett J. Sopher,[a] Miranda L. Vinay,[a] Ervin Sejdic,[b] Alexander Star*[a]

[a.] *Department of Chemistry, University of Pittsburgh, PA 15260, United States*

[b.] *Department of Electrical and Computer Engineering, University of Pittsburgh, PA 15260, United States*

Abstract

Semiconductor-enriched single-walled carbon nanotubes (s-SWCNT) have potential for application as chemiresistor for the detection of breath compounds including tetrahydrocannabinol (THC), the main psychoactive compound found in the marijuana plant. Herein we show that chemiresistor devices fabricated from s-SWCNT ink using dielectrophoresis can be incorporated into a hand-held breathalyzer with sensitivity toward THC generated from a bubbler containing analytical standard in ethanol and a heated breath sample collector that releases compounds from steel wool. The steel wool was used to capture THC from exhaled marijuana smoke. The generation of the THC from the bubbler and heated breath sample chamber was confirmed using UV-Vis absorption spectroscopy and mass spectrometry, respectively. Enhanced selectivity toward THC over more volatile breath components such as CO_2, water, ethanol, methanol, and acetone was achieved by delaying the sensor reading to allow for the desorption of these compounds from the chemiresistor surface.

Keywords: CNT, chemiresistor, tetrahydrocannabinol, THC, sensor, breath analysis, breathalyzer

Single-walled carbon nanotubes (SWCNT) are an ideal material for detecting trace concentrations of chemical[1, 2] and biological[3, 4] compounds because of their high surface area to volume ratio and their interactions with the local chemical environment can be probed by simple resistive measurements.[5] Because of their high sensitivity, low concentrations (ppb to ppm range) of endogenous and exogenous compounds in the breath,[6, 7] such as nitric oxide,[8] acetone[9] and ethanol,[10] can be detected and quantified using chemiresistors fabricated from a thin film network of SWCNT to perform breath analysis.[11] Since the sensing mechanism of nanotubes involves measuring changes in charge carrier population and charge pinning,[5] chemical sensitivity can be further enhanced by increasing the ratio between semiconducting and metallic nanotubes through various enrichment methods.[12-15] Chemiresistors fabricated from the semiconductor enriched SWCNT (s-SWCNT) have been shown to have 2 to 3 orders of magnitude higher sensitivity than chemiresistors fabricated from mixed metallic and semiconducting SWCNT.[16, 17] Herein, we show that one of the potential applications of s-SWCNT based chemiresistor is the detection of ethanol and delta-9-tetrahydrocannabinol (THC) in human breath.

THC is the main psychoactive compound found in marijuana plants.[18] When consumed in the form of vapor, edible goods, or topical agents, THC can induce a range of impaired cognitive effects including drowsiness, reduced hand-eye coordination, and blurred vision. With the legalization of marijuana, THC-containing products are becoming more widely used and available both for recreational and medical purposes, therefore the number of drivers under the influence of THC has become more prominent, increasing the public safety risk for drivers.[19] Combination of THC and ethanol intoxication has been shown to cause even higher rates of road accidents than intoxication with each component on its own.[20] Although the link between cognitive impairment and THC levels found in various bodily fluids such as urine, saliva, blood and breath is far from clearly established,[21] there is wide push by the legal system to formulate a testing protocol to measure the degree of impairment that measures the amount of THC in the driver to prevent accidents on the road.[21] The requirement for measuring impairment in drivers has brought about a need for roadside tools that measure THC in readily accessible biological

fluids such as breath[22] and saliva[23, 24] similar to how an alcohol breathalyzer can measure alcohol concentration in the breath and correlate to blood alcohol levels (BAC). Breath THC concentration has been shown to be a correlate for the time since smoking of marijuana.[22] A sensor that can measure the THC content of a breath sample can be incorporated into a breathalyzer and potentially be used as part of a roadside test protocol to measure impairment similar to how an alcohol breathalyzer functions in conjunction with field sobriety tests.

Herein, we present a chemiresistor sensor device based on a thin film of s-SWCNT with sensitivity and selectivity toward THC. Selectivity toward THC over ethanol, acetone, and humidity was achieved by focusing on the recovery portion of the chemiresistor sensing sequence, at which point the more volatile compounds had desorbed from the chemiresistor surface at a faster rate than THC. A breathalyzer prototype was then built around the chemiresistor using the open-source Arduino prototyping platform and a 3D printed case to demonstrate a proof-of-concept of how the chemiresistor could be incorporated into a breathalyzer.

Materials and Methods

Commercial unsorted single-walled carbon nanotubes (P2 SWNT, Carbon Solutions Inc.) with 33% metallic and 67% semiconducting composition and poly(9,9-di-n-dodecylfluorenyl-2,7-diyl) (PFDD) wrapped enriched semiconducting single-walled carbon nanotubes (IsoSol-S100, Raymor Industries Inc.) with 0.1% metallic and 99.9% semiconducting composition were used in this study. 1 mg/mL Δ^9-THC in methanol and 25 mg/mL Δ^9-THC in ethanol were purchased from Sigma Aldrich and diluted in 200 proof ethanol from Decon Laboratories for use in the bubbler. Additional experimental details can be found in the Supporting Information.

Bubbler Description and Calibration

THC vapor was generated using a bubbler system. The bubbler (Figure 1b) was assembled using a 250 mL Duran glass bottle, Duran GL 45 connection system caps and accessories, and 1.5 mm ID PTFE

tubing purchased from Sigma Aldrich. The inlet tubing of the bubbler was connected to Bronkhorst EL-FLOW Prestige mass flow controller (MFC), which delivered Ultra Zero Grade dry air from gas cylinders supplied by Matheson Tri-Gas at a flow rate of 500 sccm. The bubbler was filled with 50 mL of ethanol dissolved THC analytical standard (0.1 mg/mL), m-xylene (0.1 mg/mL), or olivetol (0.1 mg/mL). For generation of pure THC vapor, the ethanol from the THC/ethanol bubbler solution was evaporated off using an air aspirator vacuum pump (100 mbar) overnight leaving THC oil. To generate the synthetic human breath, the bubbler was filled with water and 0.1 vol% of ethanol and 0.1 vol% of acetone. 10.5 vol% carbon dioxide balanced in nitrogen supplied by Matheson Tri-Gas was diluted in air to generate 5.00 vol% carbon dioxide gas stream.

To calibrate the THC/ethanol bubbler, the vapor generated from the bubbler was captured on a hole punched out filter paper in a 1-dram glass vial for cumulative durations of 4.5, 9.5, 19.5, 49.5, 109.5, 229.5, or 469.5 minutes. To extract out the THC, 100 µL of ethanol was added to the vial and incubated at room temperature over-night and then placed in the freezer until the time of UV-Vis absorption measurement (250 to 350 nm).

Chemiresistor Fabrication

The 2x2 mm silicon dies with 4 pairs of interdigitated gold electrodes (IDE) were fabricated using standard photolithography processes (Figure 1a). The silicon dies were then wirebonded and potted into standard 40-pin ceramic dual in-line (DIP) packages using polydimethylsiloxane (PDMS) to secure the die and the wirebonds. Either IsoSol or P2 SWCNT were deposited as thin films on the interdigitated gold electrodes using dielectrophoresis (DEP) using a Keithley 3390 Arbitrary Waveform Generator. 5 µL of 10 µg/mL IsoSol solution in toluene or P2 in DMF was dropped on top of the silicon die. A sine wave (IsoSol: 10 V_{pp}, 100 kHz, 2 min; P2: 10 V_{pp}, 10 MHz, 1 min) was applied between the IDEs. The IsoSol deposited devices were rinsed with toluene, acetone, and water, while the P2 deposited devices rinsed with DMF and water. The devices were then annealed in an oven at 120°C for an hour to dry off any bound solvent molecules. The dielectrophoretic force generated by DEP aligns the SWCNT along the

electrical field between the gold electrodes and deposits them, forming a thin layer of SWCNT network (Figure 1a inset).[25, 26] The SWCNT thin films were characterized by Raman spectroscopy, UV-Vis-NIR spectroscopy, and AFM (Figure S1).

Vapor Sensing Experiment

Electrical conductivity of the chemiresistor was measured using Keithley Source Meter Unit (SMU) 2602B by sourcing 50 mV and measuring the current every second. The 40-pin DIP package was inserted into a 40-pin zero-insertion force (ZIF) connector, which was pin mounted on a printed circuit board (PCB). A Keithley 3706A System Switch was used to switch among the 4 devices at a rate of 0.1 seconds. The Keithley equipment and MFC were synchronized and programmed using LabView 2016 software. Five seconds before the vapor exposure, the voltage from the source meter unit (SMU) was dropped to 0 V and then brought back up to 5 V, 30 seconds after the bubbler was turned off.

Results and Discussion

THC Vapor Sensing

To determine the sensitivity of the chemiresistor to THC, the THC oil and THC/ethanol bubbler had to be first calibrated. The amount of THC vapor generated by the bubbler was quantified by taking the absorbance at 276 nm of known concentrations of THC/ethanol solutions (Figure 1c) and comparing to the absorbance at 276 nm of the THC vapor captured on and extracted from a filter paper (Figures S2a-d). The THC vapor generated by the bubbler was assumed to be 100% captured and retained by the filter paper and the 1-dram vial during the THC vapor collection. For the pure THC oil vapor generation, the attempted UV-Vis absorption-based calibration (Figures S2a and S2b) indicated that THC vapor was not being delivered consistently in a linearly proportional manner to the duration of the vapor collection. However, for the THC/ethanol bubbler, the UV-Vis based bubbler calibration showed delivery of THC vapor linearly proportional to the bubbler on time. The UV-Vis absorption-based calibration was more quantitative and reliable than a qualitative colorimetric based on Fast Blue B dye, which yields red to

violet color in the presence of THC (SI Section 3 and Figure S2e).[27] The THC/ethanol bubbler system approximately generates 210 ng of THC per hour.

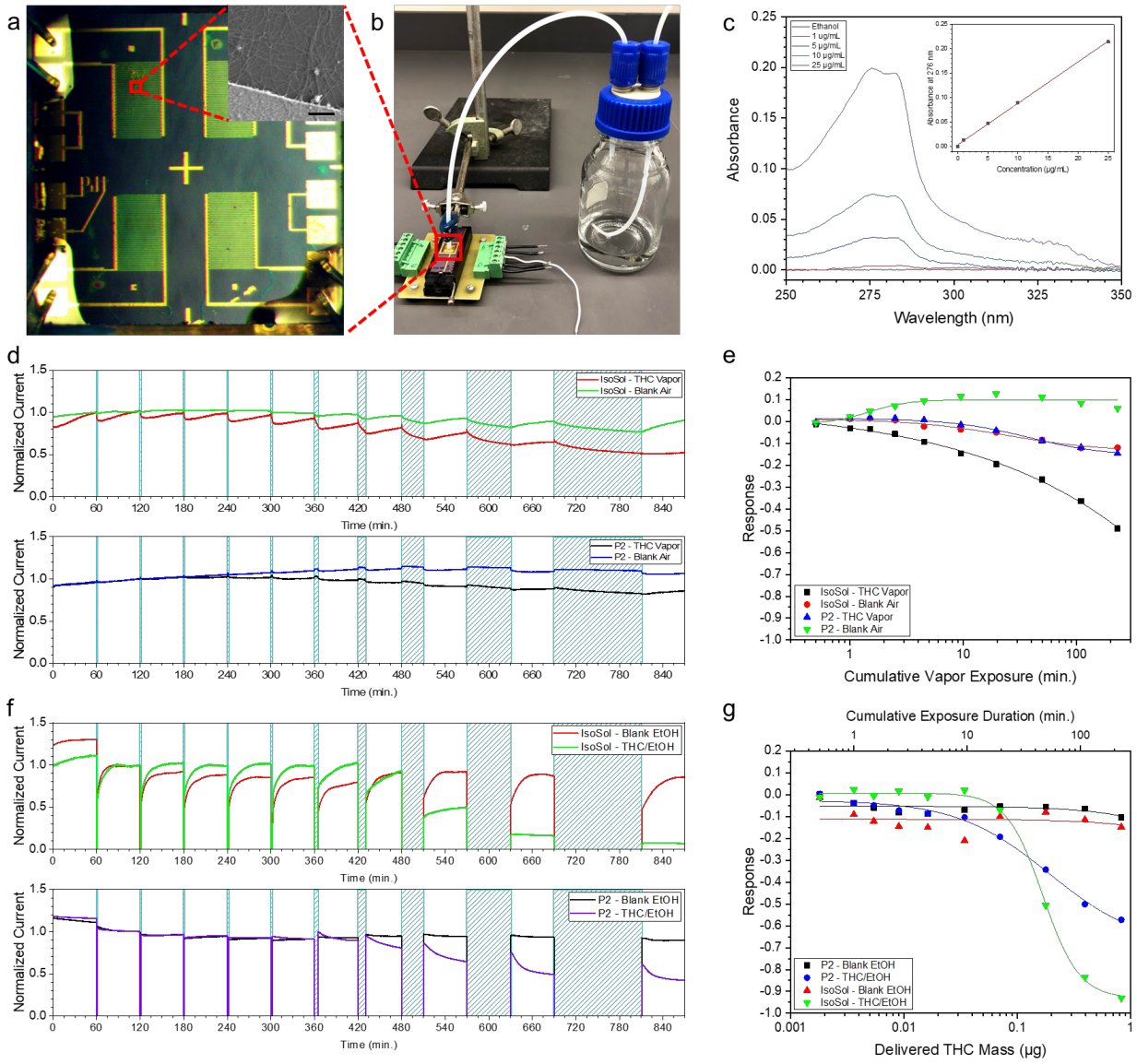

Figure 1. THC sensing in the gas phase. (a) Optical image of a 2x2 mm silicon chip with four sets of interdigitated gold electrodes. Inset: SEM micrograph of IsoSol S-100 nanotube network deposited via DEP between gold electrodes (scale bar = 500 nm). (b) Image of the bubbler with the outlet Teflon tubing clamped directly above the packaged silicon chip. (c) UV-Vis absorption spectra of THC/ethanol standards of known concentration. Inset: Calibration curve of THC/ethanol standards calibrated to the absorption at

276 nm. (d) THC vapor sensing data for IsoSol-S100 and P2 nanotube deposited devices from vapor generated from pure THC oil. The light blue dashed boxes mark the time period when the air flow was turned on. The chemiresistors have higher relative response and less relative recovery when exposed to THC vapor compared to air. (e) The calibration plots of the chemiresistors calibrated to the cumulative vapor exposure. The responses can be fit with a Hill-Langmuir equation. (f) Vapor sensing data for the IsoSol-S100 and P2 nanotube deposited devices. The light blue dashed boxes indicate the time period when the bubbler was turned on and the sensor voltage was turned off to 0 V. The normalized current after vapor exposure have different relative recovery depending on the constituents of the exposed vapor. (g) The calibration plots of the chemiresistors calibrated to the calculated THC mass derived from (c). The response profiles can be fit with the Hill-Langmuir equation.

The current measurements taken by the SMU and the system switch (Figure 1d) were normalized to the current at the 60 minute mark to account for day-to-day variation in chemiresistor conductivity caused by changes in the charge state of the silicon dioxide substrate due to variable humidity levels[28-31] and device-to-device variation caused by the variance in the density of SWCNT network that was deposited, defects in the SWCNT, damage in the gold interdigitated electrodes.[32, 33] The chemiresistor was exposed to THC vapor generated from the bubbler or blank air for durations of 0.5 (3 consecutive times), 1, 2, 5, 10, 30, 60, and 120 minutes. The difference in relative response and relative recovery for the THC sensing data compared to blank air data (Figure 1e) indicated THC vapor was likely being delivered to the chemiresistor, however as previously stated, the attempted UV-Vis calibration (Figure S2c and S2d) showed inconsistent delivery of THC. The THC/ethanol bubbler was used for further characterization of the chemiresistor due to the quantifiable linear rate of THC vapor generation.

For the ethanol-based bubbler studies (Figure 1f), the current measurements were normalized to the current at the 120-minute mark so that the first 0.5 minute exposure acted as a priming step to account for the irreversible adsorption of ethanol in addition to accounting for the day-to-day variability of the chemiresistor. A downside to using the ethanol-based bubbler was the devices showing inconsistent

response when exposed to saturated ethanol vapor (Figure S3) with some devices showing increases in conductivity, while others showed decreases in conductivity. By halting the applied bias during and 30 seconds after the vapor exposure, the SWCNT chemiresistors showed consistent decrease in conductivity after exposure to saturated ethanol vapor (Figure 1f) as expected from previously reported studies.[34]

The decrease in conductivity of the chemiresistor can be attributed to ethanol binding to PFDD polymer wrapping around the SWCNT and causing the polymer to swell, thereby increasing the inter-nanotube tunneling distance,[35, 36] adsorbing to the defect sites on the surface of nanotubes and donating its electrons,[37-39] adsorbing to the underlying silicon dioxide substrate and changing its potential,[34] and/or binding near s-SWCNT/Au electrode junctions and modulating the Schottky barrier, which have all shown to be responsible for the changes in conductivity of SWCNT chemiresistors.[5] When the bubbler is turned off, the conductivity partially recovers on the order of approximately an hour as the ethanol desorbs. However, when the sensing experiment was conducted with THC containing ethanol solution, the chemiresistors never fully recovered to their nominal conductivity, indicating strong adsorption of the THC molecule even an hour after the vapor exposure (Figure 1f and 1g).

The typical approach to chemiresistor sensing analysis focuses on the relative response, which is defined as the change in the sensor current before (I_0) and after (I_t) analyte exposure. (Eq 1)

$$Relative\ response\ = \frac{I_t - I_0}{I_0} \quad \text{(Eq 1)}$$

However, when the chemiresistor is exposed to both THC and ethanol vapor, the dominant signal in the relative response is due to adsorption of ethanol molecules. The range of relative response (-0.39 to -0.56) to saturated ethanol vapor for all the exposure durations is just below the relative response (-0.61) to 49.5 minutes of accumulated exposure to THC and ethanol vapors (Figure S4). Before this exposure duration, not enough THC has accumulated on the nanotubes to generate a strong enough signal to distinguish between THC/ethanol from pure ethanol vapor. Instead, the focus of the analysis was shifted to comparing the conductivity of the sensor after recovery from the first 0.5-minute priming step (current at t

= 120 minutes) to approximately 50 minutes into the recovery sequence of each subsequence exposure when most of the ethanol had desorbed from the surface of the chemiresistor (Figure 1g). Any change in the current before the vapor exposure and after ethanol desorption is therefore due to the accumulation of THC. This relative change in current will be referred to as the sensor response.

When comparing the sensor response to blank ethanol vapor compared to THC/ethanol vapor, the recovery point of the chemiresistor is significantly lower when the chemiresistor was exposed to combined ethanol and THC vapor compared to pure ethanol vapor (Figure 1g). This difference in the final recovery point can be attributed to the higher volatility of ethanol (78°C boiling point for ethanol versus 157°C for THC). The shift to comparing the recovery points after vapor exposure improves the selectivity and sensitivity of the sensor toward THC as observed by the smaller relative change in current for blank ethanol vapors in Figure 1g compared to Figure S4.

To compare the performance of the s-SWCNT chemiresistor, devices were fabricated from commercial unsorted single-walled carbon nanotubes (P2-SWNT, Carbon Solutions Inc.). P2 SWCNT were also tested for ethanol and THC sensitivity. The P2 based chemiresistor also showed inconsistent spikes in current when the sensor was held at a constant bias and then exposed to saturated ethanol vapor (Figure S5). Interestingly, the s-SWCNT (IsoSol) devices showed much higher sensitivity toward ethanol compared to P2 devices. When the ethanol vapor exposure is stopped, and the sensor bias is reapplied, the P2 devices almost fully recover within 30 seconds. Whereas the s-SWCNT devices require 30 minutes before the devices are recovered. The PFDD wrapping around the s-SWCNT binds ethanol molecules and swell[40] increasing the nanotube-to-nanotube distance in the s-SWCNT network.[41] The result is a decrease in conductivity of the chemiresistor and slow recovery as the ethanol molecules desorb from the hydrophobic polymer. However, the 30 minute recovery is not expected to be required in the implementation of the chemiresistor in a breathalyzer since breath samples will contain only few hundred ppm levels of ethanol at most.

As expected, the IsoSol devices had higher sensitivity toward THC (Figure 1g) due to the higher proportion of semiconducting SWCNT (>99.9% versus ~66%).[41-43] The higher sensitivity of the s-SWCNT enriched IsoSol devices can be explained by its much smaller off current. To illustrate this point, the FET transfer curves of both P2 and IsoSol devices were measured in water before and after incubation with THC saturated water (Figures S6a and S6b). The relative change in drain current (I_d) at -0.205 V gate voltage (V_g) vs Ag/AgCl in 3.5 M KCl, which corresponds to 0 V_g vs NHE, is much higher for IsoSol device (-0.937) compared to the P2 device (-0.158). However, the shift in threshold voltage is the same for both types of nanotubes.

The responses of both P2 and IsoSol based chemiresistors to THC vapor could be fit to the Hill-Langmuir equation, which indicates Langmuir isotherm adsorption behavior.

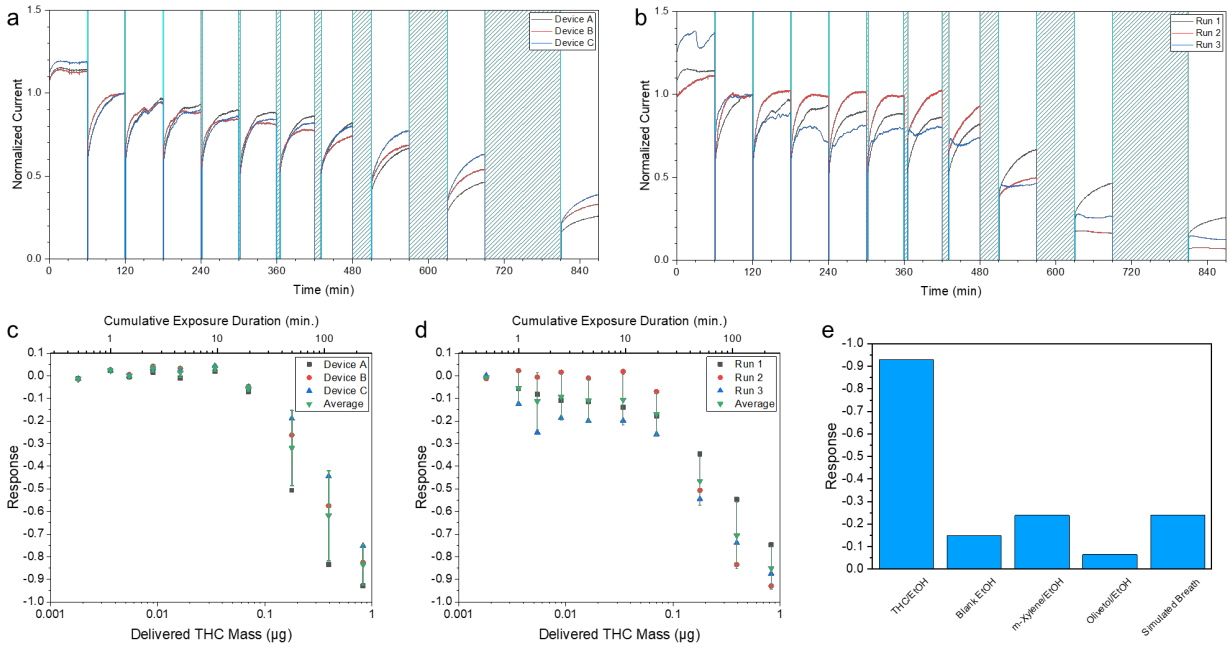

Figure 2. Chemiresistor variability, reproducibility, and cross-sensitivity. (a) THC sensing data from three functioning devices on a single chip. (b) THC sensing data from three repeated runs of a single device. (c) Calibration plot for panel a, including the average response and standard deviation of the three devices. (d) Calibration plot for panel d, including the average response and standard deviation of the

three runs. (e) Cross sensitivity of the sensor to similarly structured compounds and commonly found breath components.

For additional sensor characterization, the device-to-device variability was quantified (Figures 2a and 2c). The highest measured variability in response of chemiresistor devices was for the 0.394 μg of the calculated THC delivery. The devices showed up to ±0.25 relative standard deviation in variability. CNT devices fabricated from DEP are known to have device-to-device variability.[32, 33] In addition, the bubbler setup had the tendency to deliver higher concentration of THC along the inner diameter of the outlet tubing (Figure S2c). This implies the THC is not delivered homogeneously to the four sensor devices on the silicon chip. To demonstrate the reusability of the chemiresistor, multiple sensing experiments were done using a single sensor chip (Figures 2b and 2d). Between each sensing run, the chip was rinsed with isopropyl alcohol and dried in the oven at 120°C for 1 hour. The same device showed up to ±0.15 standard deviation in variability run-to-run further highlighting the heterogeneous nature of the bubbler delivery in addition to day-to-day variations.

Scheme 1. (-)-Δ^9-tetrahydrocannabinol (THC), olivetol, and m-xylene.

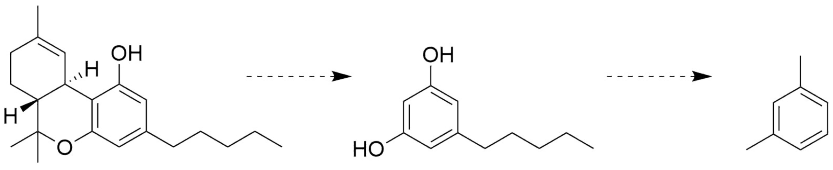

In addition to ethanol, the sensor was tested for cross sensitivity (Figure S7) to compounds (Scheme 1) with similar structure to THC (m-xylene and olivetol) with similar bubbler concentration (0.1 mg/mL) and commonly found breath compounds (water, ethanol, acetone, carbon dioxide) at close to physiologically relevant concentrations. The chemiresistor showed the higher sensitivity to THC, 157°C BP, over the more volatile m-xylene, 139°C BP, (Figure 2e). Olivetol, which is the synthetic precursor to THC, has a much higher boiling point (BP = 313°C) so direct comparison of cross sensitivity was not

reliable. The chemiresistor also had higher sensitivity to the simulated breath, which was composed of saturated water vapor, 5 vol% carbon dioxide in air and trace amounts of acetone and ethanol.

To potentially improve the sensitivity and selectivity of the chemiresistor, both non-linear and linear classification algorithms: random forest (RF), k-nearest neighbor (kNN), and support vector machine classifier, with linear kernel(SVC), were trained to classify the recovery portion of sensing data into two classes, THC or Non-THC. RF is an ensemble algorithm based on a decision tree, which inherits the strong classification power from decision tree algorithm but is more robust. kNN is a simple but strong classification algorithm, which computes the Euclidean distance between the unknown sample and each observation in the dataset. The final classification is determined by the number of voters in each class. SVC is an algorithm that maximizes the distance between the support vector of each class and the boundary. It is powerful for classifying any linearly separable data.

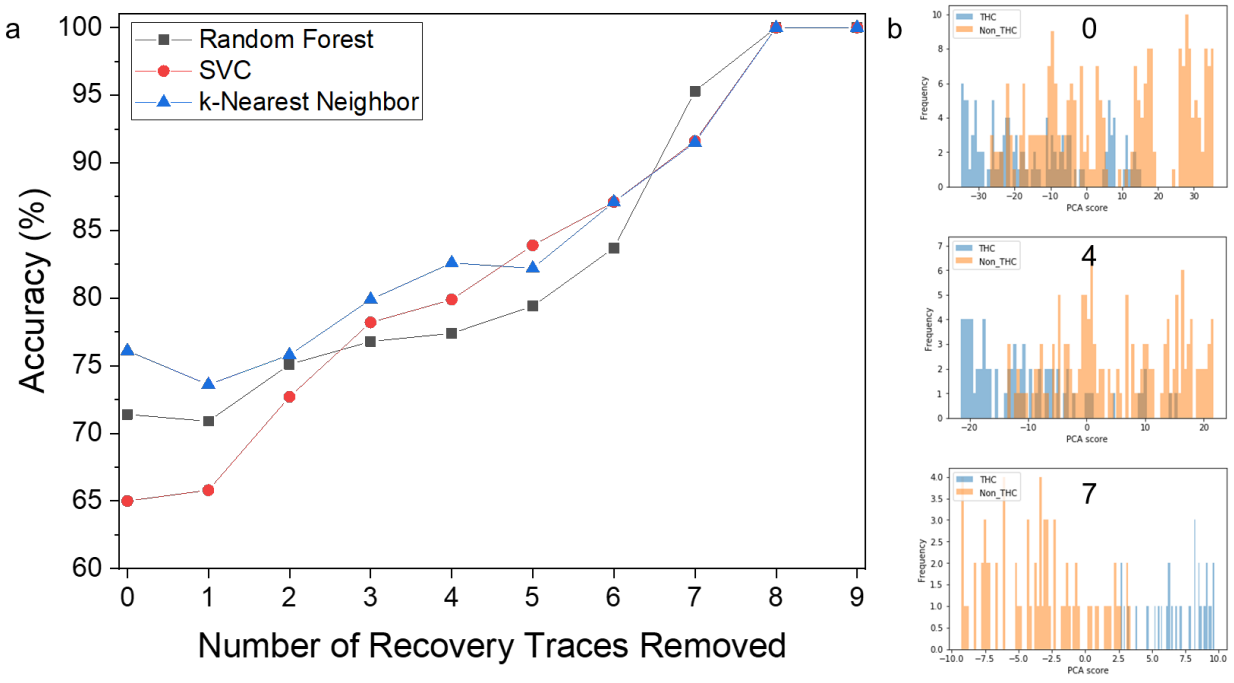

Figure 3. (a) Accuracies of the models from three classification algorithms versus the number of recovery traces removed. (b) 1-Dimensional distribution of two classes of data, THC vs non-THC, after processing by t-SNE followed by PCA.

The prediction accuracy of each algorithm was plotted against the number of the recoveries that were removed from the dataset (Figure 3a). The models' accuracies started improving above 80% after the removal of first 5 recoveries. If we remove the first 7 recoveries, the accuracies increase to above 90% with the highest accuracy being above 95% from RF, which is consistent with the calibration curve generated in Figure 1f as well as the data distribution (Figures 3b and S7).

t-SNE (t-distributed stochastic neighbor embedding) is a non-linear dimensionality reduction algorithm well suited for reducing the high dimension data to low dimension for visualization purposes. It computes the distribution between each original data point at high dimension, and creates a similar distribution at low dimension, the difference between the two distributions are minimized with Kullback–Leibler divergence. In 2D t-SNE plots, most of the data points are along the diagonal, therefore, we extracted the diagonal information using principal component analysis (PCA) and plotted it in 1D histogram (Figure#, SI). As more recoveries from sensing data are removed, the two classes on the histograms become more separable.

Breathalyzer Prototyping

To demonstrate a proof-of-concept THC breathalyzer, a prototype was fabricated using a 3D printed housing (Figures 4a, 4b, and 4c), which enclosed an Arduino Uno microcontroller that detected resistance changes in the chemiresistor and displayed the changes on to an LCD screen (Figure 4b). To detect the resistance changes in the chemiresistor, the circuitry of the prototype was designed so that the chemiresistor and a reference potentiometer was connected in a voltage divider network (Figure 4d). When the resistance of the chemiresistor changes, the voltage change across the chemiresistor can be measured relative to the voltage across the potentiometer and the 5 V reference voltage (V_{in}) generated by the microcontroller (Figure S9). The voltage measured across the chemiresistor is then converted to a 10-bit number (i.e., 1024 possible output codes) by the Arduino Uno microcontroler's analog-to-digital (ADC) converter. The ADC's resolution is 4.88 mV using a 5 V reference voltage (e.g., a conversion value of 512 corresponds to 2.5 V, while a conversion value of 1023 corresponds to approximately 4.995

V). In a voltage divider, the maximum change in the voltage magnitude across one resistor is observed when the two resistors in the network start approximately at the same resistance. To account for the day-to-day and device-to-device variation of the chemiresistor, a 100 kΩ potentiometer was used as variable reference resistor that could be dialed to match the nominal resistance of the chemiresistor.

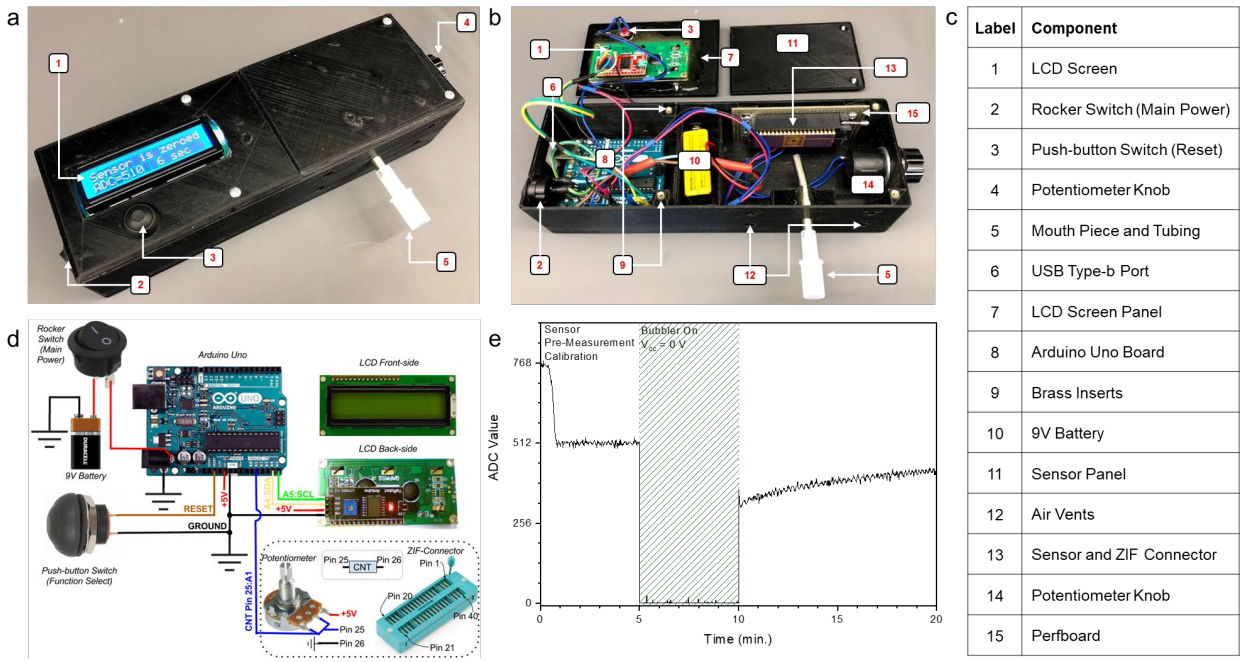

Label	Component
1	LCD Screen
2	Rocker Switch (Main Power)
3	Push-button Switch (Reset)
4	Potentiometer Knob
5	Mouth Piece and Tubing
6	USB Type-b Port
7	LCD Screen Panel
8	Arduino Uno Board
9	Brass Inserts
10	9V Battery
11	Sensor Panel
12	Air Vents
13	Sensor and ZIF Connector
14	Potentiometer Knob
15	Perfboard

Figure 4. Chemiresistor incorporation into a prototype breathalyzer (a). External image of the fully assembled breathalyzer prototype. (b) Internal assembly image of the prototype with unscrewed sensor panel and LCD screen panel. (c) Labels for figures a and b. (d) Internal circuitry of the prototype. (e) THC sensing data acquired using the prototype. The drop in ADC value in the first minute mark is due to the winding of the potentiometer to balance the voltage divider.

Since Arduino Uno board (Figure 4d) outputs 5 V, and its analog-to-digital converter has a reference voltage of 5 V, the chemiresistor was tested with the Keithley setup at 5 V. Similar to the experiments conducted at 50 mV bias, the sensing experiments conducted at the higher supply voltage caused current spikes and inconsistent recovery profile possibly due to electrochemical reactions occurring on the nanotube or gold electrode surface (Figure S10). The inconsistent responses were

resolved by dropping the sensor supply voltage to 0 V during vapor exposure (Figures S11a and S11c). The normalized current traces show the drop in the current to 0 corresponding to the exposure time frames. Two seconds after the vapor exposure stops, the supply voltage is stepped back up to 5 V. The calibration plot (Figures S11b and S11d) derived from ethanol and THC/ethanol sensing experiment showed comparable sensitivity to THC even at the higher supply voltage. This shows that the chemiresistor can function at a wide range of voltages including 50 mV supplied by the SMU and 5 V supplied by the Arduino prototype platform.

The microcontroller was programmed to resemble the sensing experiment done to characterize the chemiresistor. In the first 5 minutes, the potentiometer is dialed to match the nominal resistance of the chemiresistor, and any drifts in the voltage across the chemiresistor is measured (Figure 4e). In the following 5 minutes, the voltage output from the microcontroller is dropped to 0 V and the chemiresistor is then exposed to the sample gas. After the 5-minute exposure, the voltage is stepped back up to 5 V and the chemiresistor recovery profile is collected.

Prototype Testing

To demonstrate the potential use of the THC chemiresistor as a breathalyzer, THC analytical standards and captured breath and smoke samples from a volunteer were analyzed using the prototype and compared to a mass spectrometer. A chamber heated to 120°C with nitrogen gas inlet and outlet were used to release the captured THC vapor. For the analytical standards, a steel wool (half-inch diameter) soaked with either blank methanol or THC dissolved in methanol (0.1mg/mL) was air dried and then placed into the heated chamber. The chemiresistor in the prototype showed a greater drop in ADC values, which corresponds to larger decrease in conductivity, for THC/methanol then just methanol alone. The response to blank methanol is due to the residual methanol on the steel wool evaporating in the heated chamber (Figure 5a). At approximately the 12.5-minute mark, the residual methanol has completely evaporated leading to the early recovery of the sensor. However, the THC/methanol sample continued to

respond to the deposited THC. The presence of THC in the THC/methanol standard was verified using a mass spectrometer (Figure 5b).

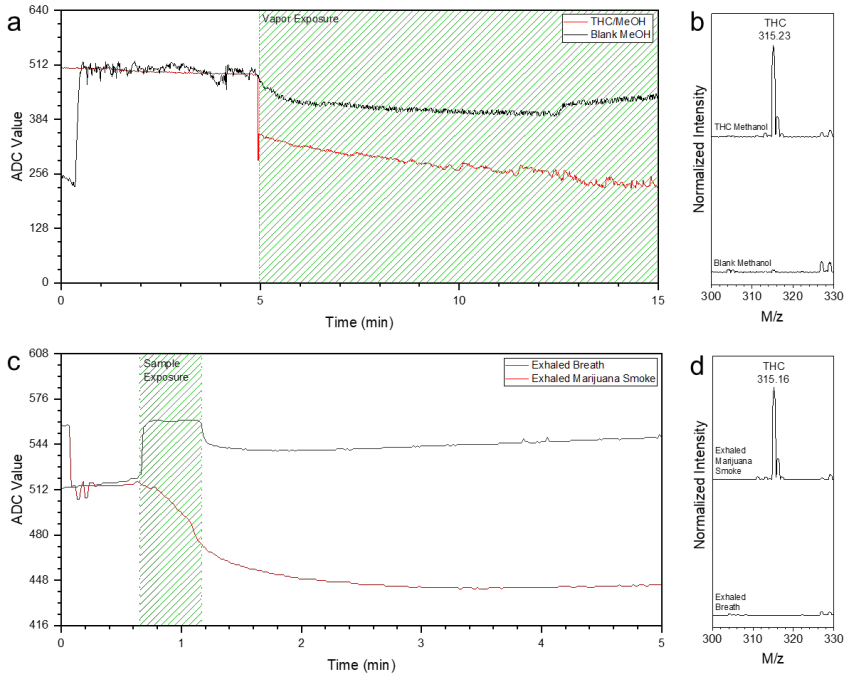

Figure 5. Captured breath and smoke analysis. (a) THC vapor and methanol vapor sensing data collected using the prototype. (b) Mass spectra of the vapors generated from the THC/methanol standard and blank methanol. (c) Vapors from captured marijuana smoke and exhaled breath analyzed using the prototype. (d) Mass spectra of the volatile compounds captured from exhaled breath and exhaled smoke.

In addition to the standards, THC captured on the steel wool from exhaled marijuana smoke was compared to a captured breath sample without any THC. To collect the blank exhaled breath sample, a volunteer exhaled into a breath tube stuffed with the steel wool. The volunteer then exhaled marijuana smoke during a smoking session into the breath tube and steel wool. The steel wool samples were then removed and inserted into the heated chamber. The sensor showed a response, measured as a decrease in the ADC value, only to the exhaled smoke sample (Figure 5c). The sensor showed increase in ADC value to the blank breath sample. This positive response may be due to the number of exogenous and

endogenous compounds found in exhaled breath.[44, 45] The presence of the THC in the captured smoke sample was verified using the mass spectrometer compared to captured blank breath sample (Figure 5d).

For potential field application of the THC chemiresistor and the prototype breathalyzer,

Conclusion

A chemiresistor fabricated with DEP deposited s-SWCNT was demonstrated to show the capability to detect deposited THC with a detection limit of 0.163 ng (using S/N = 3), the main psychoactive compound found in the marijuana plant. To increase the selectivity of the chemiresistor toward THC over more volatile compounds such as ethanol and to account for the higher drive voltage of the Arduino prototyping platform, the sensor was calibrated by focusing on the recovery portion of current versus time traces. The chemiresistor was shown to function when incorporated into a prototype breathalyzer. With the increase in THC containing products becoming more widely available and consumed, THC sensors could potentially find applications in public safety and quality control areas.

Corresponding Author

Alexander Star, PhD

E-mail: astar@pitt.edu.

Acknowledgement

This work at the University of Pittsburgh was supported by Chancellor's Innovation Fund and Pitt Ventures First Gear program (NSF 1734751). Raman characterization was completed through the assistance of a ONR (N000141410765) grant. We thank Characterization Facility (NFCF) at the University of Pittsburgh for access to the SEM instrumentation. We thank Dr. Jianfu Ding and Dr. Patrick Malenfant at the National Research Council of Canada for providing high-purity semiconducting single-walled carbon nanotubes.

Supporting Information

The Supporting Information is available free of charge on the ACS Publications website at DOI:

Experimental section, SWCNT spectroscopic and AFM characterization, vapor sensing data at constant voltage, ethanol and THC vapor relative response calibration, vapor sensing data at 5 V, prototype circuitry, housing, and software description

References

(1) Kong, J.; Franklin, N. R.; Zhou, C. W.; Chapline, M. G.; Peng, S.; Cho, K. J.; Dai, H. J. Nanotube molecular wires as chemical sensors. *Science,* **2000**, *287*, 622-625.
(2) Li, J.; Lu, Y.; Ye, Q.; Cinke, M.; Han, J.; Meyyappan, M. Carbon Nanotube Sensors for Gas and Organic Vapor Detection. *Nano Lett.* **2003**, *3*, 929-933.
(3) Besteman, K.; Lee, J.-O.; Wiertz, F. G. M.; Heering, H. A.; Dekker, C. Enzyme-Coated Carbon Nanotubes as Single-Molecule Biosensors. *Nano Lett.* **2003**, *3*, 727-730.
(4) Chen, R. J.; Zhang, Y.; Wang, D.; Dai, H. Noncovalent Sidewall Functionalization of Single-Walled Carbon Nanotubes for Protein Immobilization. *J. Am. Chem. Soc.* **2001**, *123*, 3838-3839.
(5) Schroeder, V.; Savagatrup, S.; He, M.; Lin, S.; Swager, T. M. Carbon Nanotube Chemical Sensors. *Chem. Rev.* **2019**, *119*, 599-663.
(6) Ellis, J. E.; Star, A. Carbon Nanotube Based Gas Sensors toward Breath Analysis. *ChemPlusChem,* **2016**, *81*, 1248-1265.
(7) Broza, Y. Y.; Vishinkin, R.; Barash, O.; Nakhleh, M. K.; Haick, H. Synergy between nanomaterials and volatile organic compounds for non-invasive medical evaluation. *Chem. Soc. Rev.* **2018**, *47*, 4781-4859.
(8) Kuzmych, O.; Allen, B. L.; Star, A. Carbon nanotube sensors for exhaled breath components. *Nanotechnology,* **2007**, *18*, DOI: 10.1088/0957-4484/18/37/375502.
(9) Ding, M.; Sorescu, D. C.; Star, A. Photoinduced charge transfer and acetone sensitivity of single-walled carbon nanotube-titanium dioxide hybrids. *J. Am. Chem. Soc.* **2013**, *135*, 9015-9022.
(10) Ellis, J. E.; Green, U.; Sorescu, D. C.; Zhao, Y.; Star, A. Indium Oxide-Single-Walled Carbon Nanotube Composite for Ethanol Sensing at Room Temperature. *J. Phys. Chem. Lett.* **2015**, *6*, 712-717.
(11) Chen, K.; Gao, W.; Emaminejad, S.; Kiriya, D.; Ota, H.; Nyein, H. Y.; Takei, K.; Javey, A. Printed Carbon Nanotube Electronics and Sensor Systems. *Adv. Mater.* **2016**, *28*, 4397-4414.
(12) Ding, J.; Li, Z.; Lefebvre, J.; Cheng, F.; Dubey, G.; Zou, S.; Finnie, P.; Hrdina, A.; Scoles, L.; Lopinski, G. P.; Kingston, C. T.; Simard, B.; Malenfant, P. R. Enrichment of large-diameter semiconducting SWCNTs by polyfluorene extraction for high network density thin film transistors. *Nanoscale,* **2014**, *6*, 2328-2339.
(13) Wang, J.; Nguyen, T. D.; Cao, Q.; Wang, Y.; Tan, M. Y.; Chan-Park, M. B. Selective Surface Charge Sign Reversal on Metallic Carbon Nanotubes for Facile Ultrahigh Purity Nanotube Sorting. *ACS Nano,* **2016**, *10*, 3222-3232.
(14) Arnold, M. S.; Green, A. A.; Hulvat, J. F.; Stupp, S. I.; Hersam, M. C. Sorting carbon nanotubes by electronic structure using density differentiation. *Nat. Nanotechnol.* **2006**, *1*, 60-65.
(15) Ding, J.; Li, Z.; Lefebvre, J.; Cheng, F.; Dunford, J. L.; Malenfant, P. R.; Humes, J.; Kroeger, J. A hybrid enrichment process combining conjugated polymer extraction and silica gel adsorption for high purity semiconducting single-walled carbon nanotubes (SWCNT). *Nanoscale,* **2015**, *7*, 15741-15747.
(16) Ganzhorn, M.; Vijayaraghavan, A.; Dehm, S.; Hennrich, F.; Green, A. A.; Fichtner, M.; Voigt, A.; Rapp, M.; von Lohneysen, H.; Hersam, M. C.; Kappes, M. M.; Krupke, R. Hydrogen sensing with diameter- and chirality-sorted carbon nanotubes. *ACS Nano,* **2011**, *5*, 1670-1676.

(17) Xiao, M.; Liang, S.; Han, J.; Zhong, D.; Liu, J.; Zhang, Z.; Peng, L. Batch Fabrication of Ultrasensitive Carbon Nanotube Hydrogen Sensors with Sub-ppm Detection Limit. *ACS Sens.* **2018**, *3*, 749-756.
(18) Gaoni, Y.; Mechoulam, R. Isolation, Structure, and Partial Synthesis of an Active Constituent of Hashish. *J. Am. Chem. Soc.* **1964**, *86*, 1646-1647.
(19) Berning, A.; Compton, R.; Wochinger, K. Drug and Alcohol Crash Risk (DOT HS 812 117). Washington, DC: National Highway Traffic Safety Administration. **2015**,
(20) Ramaekers, J. G.; Robbe, H. W. J.; O'Hanlon, J. F. Marijuana, alcohol and actual driving performance. *Hum. Psychopharmacol.* **2000**, *15*, 551-558.
(21) Hartman, R. L.; Huestis, M. A. Cannabis effects on driving skills. *Clin. Chem.* **2013**, *59*, 478-492.
(22) Himes, S. K.; Scheidweiler, K. B.; Beck, O.; Gorelick, D. A.; Desrosiers, N. A.; Huestis, M. A. Cannabinoids in exhaled breath following controlled administration of smoked cannabis. *Clin. Chem.* **2013**, *59*, 1780-1789.
(23) Lee, J. R.; Choi, J.; Shultz, T. O.; Wang, S. X. Small Molecule Detection in Saliva Facilitates Portable Tests of Marijuana Abuse. *Anal. Chem.* **2016**, *88*, 7457-7461.
(24) Ramaekers, J. G.; Moeller, M. R.; van Ruitenbeek, P.; Theunissen, E. L.; Schneider, E.; Kauert, G. Cognition and motor control as a function of Delta9-THC concentration in serum and oral fluid: limits of impairment. *Drug Alcohol Depend.* **2006**, *85*, 114-122.
(25) Vijayaraghavan, A.; Blatt, S.; Weissenberger, D.; Oron-Carl, M.; Hennrich, F.; Gerthsen, D.; Hahn, H.; Krupke, R. Ultra-large-scale directed assembly of single-walled carbon nanotube devices. *Nano Lett.* **2007**, *7*, 1556-1560.
(26) Krupke, R.; Linden, S.; Rapp, M.; Hennrich, F. Thin Films of Metallic Carbon Nanotubes Prepared by Dielectrophoresis. *Adv. Mater.* **2006**, *18*, 1468-1470.
(27) Nascimento, I. R.; Costa, H. B.; Souza, L. M.; Soprani, L. C.; Merlo, B. B.; Romão, W. Chemical identification of cannabinoids in street marijuana samples using electrospray ionization FT-ICR mass spectrometry. *Anal. Methods,* **2015**, *7*, 1415-1424.
(28) Kim, W.; Javey, A.; Vermesh, O.; Wang, Q.; Li, Y.; Dai, H. Hysteresis Caused by Water Molecules in Carbon Nanotube Field-Effect Transistors. *Nano Lett.* **2003**, *3*, 193-198.
(29) Lin, H.; Tiwari, S. Localized charge trapping due to adsorption in nanotube field-effect transistor and its field-mediated transport. *Appl. Phys. Lett.* **2006**, *89*, DOI: 10.1063/1.2337104.
(30) Lee, J. S.; Ryu, S.; Yoo, K.; Choi, I. S.; Yun, W. S.; Kim, J. Origin of Gate Hysteresis in Carbon Nanotube Field-Effect Transistors. *J. Phys. Chem. C,* **2007**, *111*, 12504-12507.
(31) Cao, Q.; Han, S. J.; Penumatcha, A. V.; Frank, M. M.; Tulevski, G. S.; Tersoff, J.; Haensch, W. E. Origins and characteristics of the threshold voltage variability of quasiballistic single-walled carbon nanotube field-effect transistors. *ACS Nano,* **2015**, *9*, 1936-1944.
(32) Hu, L.; Hecht, D. S.; Gruner, G. Carbon nanotube thin films: fabrication, properties, and applications. *Chem. Rev.* **2010**, *110*, 5790-5844.
(33) Chen, J.; Kumar, S. Variability in Output Characteristics of Single-Walled Carbon Nanotube Thin-Film Transistors. *IEEE Trans. Nanotechnol.* **2018**, *17*, 353-361.
(34) Someya, T.; Small, J.; Kim, P.; Nuckolls, C.; Yardley, J. T. Alcohol Vapor Sensors Based on Single-Walled Carbon Nanotube Field Effect Transistors. *Nano Lett.* **2003**, *3*, 877-881.
(35) Li, C.; Thostenson, E. T.; Chou, T.-W. Dominant role of tunneling resistance in the electrical conductivity of carbon nanotube–based composites. *Appl. Phys. Lett.* **2007**, *91*, DOI: 10.1063/1.2819690.
(36) Wei, C.; Dai, L.; Roy, A.; Tolle, T. B. Multifunctional chemical vapor sensors of aligned carbon nanotube and polymer composites. *J. Am. Chem. Soc.* **2006**, *128*, 1412-1413.
(37) Robinson, J. A.; Snow, E. S.; Badescu, S. C.; Reinecke, T. L.; Perkins, F. K. Role of defects in single-walled carbon nanotube chemical sensors. *Nano Lett.* **2006**, *6*, 1747-1751.
(38) Salehi-Khojin, A.; Khalili-Araghi, F.; Kuroda, M. A.; Lin, K. Y.; Leburton, J. P.; Masel, R. I. On the sensing mechanism in carbon nanotube chemiresistors. *ACS Nano* **2011**, *5*, 153-158.

(39) Anoshkin, I. V.; Nasibulin, A. G.; Mudimela, P. R.; He, M.; Ermolov, V.; Kauppinen, E. I. Single-walled carbon nanotube networks for ethanol vapor sensing applications. *Nano Research* **2012**, *6*, 77-86.
(40) Huang, L.; Huang, X.; Sun, G.; Gu, C.; Lu, D.; Ma, Y. Study of β phase and Chains Aggregation Degrees in Poly(9,9-dioctylfluorene) (PFO) Solution. *J. Phys. Chem. C* **2012**, *116*, 7993-7999.
(41) Ishihara, S.; O'Kelly, C. J.; Tanaka, T.; Kataura, H.; Labuta, J.; Shingaya, Y.; Nakayama, T.; Ohsawa, T.; Nakanishi, T.; Swager, T. M. Metallic versus Semiconducting SWCNT Chemiresistors: A Case for Separated SWCNTs Wrapped by a Metallosupramolecular Polymer. *ACS Appl. Mater. Interfaces,* **2017**, *9*, 38062-38067.
(42) Roberts, M. E.; LeMieux, M. C.; Bao, Z. Sorted and aligned single-walled carbon nanotube networks for transistor-based aqueous chemical sensors. *ACS Nano,* **2009**, *3*, 3287-3293.
(43) Zhao, W.; Fam, D. W.; Yin, Z.; Sun, T.; Tan, H. T.; Liu, W.; Tok, A. I.; Boey, Y. C.; Zhang, H.; Hng, H. H.; Yan, Q. A carbon monoxide gas sensor using oxygen plasma modified carbon nanotubes. *Nanotechnology,* **2012**, *23*, DOI: 10.1088/0957-4484/23/42/425502.
(44) de Lacy Costello, B.; Amann, A.; Al-Kateb, H.; Flynn, C.; Filipiak, W.; Khalid, T.; Osborne, D.; Ratcliffe, N. M. A review of the volatiles from the healthy human body. *J. Breath Res.* **2014**, *8*, DOI: 10.1088/1752-7155/8/1/014001.
(45) Miekisch, W.; Schubert, J. K.; Noeldge-Schomburg, G. F. Diagnostic potential of breath analysis--focus on volatile organic compounds. *Clin. Chim. Acta.* **2004**, *347*, 25-39.

TOC graphic

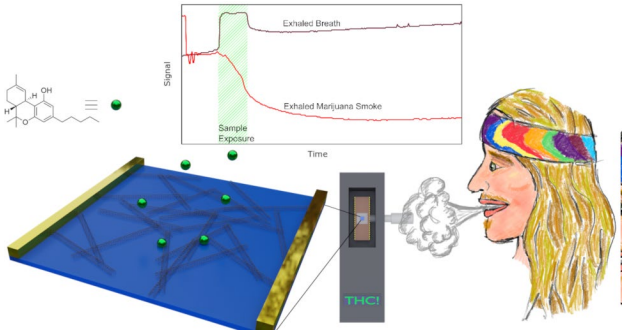

Supporting Information

Tetrahydrocannabinol (THC) Detection using Semiconductor-enriched Single-Walled Carbon Nanotube Chemiresistors

Sean I. Hwang,[a] Nicholas G. Franconi,[b] Michael A. Rothfuss,[b] Kara Bocan,[b] David L. White,[a] Seth C. Burkert,[a] Brett Sopher,[a] Miranda Vinay,[a] Ervin Sejdic,[b] Alexander Star*[a]

[a.] *Department of Chemistry, University of Pittsburgh, PA 15260, United States*

[b.] *Department of Electrical and Computer Engineering, University of Pittsburgh, PA 15260, United States*

Table of Contents

Experimental Procedures

1. Chemicals

Commercial unsorted single-walled carbon nanotubes (P2-SWNT, Carbon Solutions Inc.) and semiconducting single-walled carbon nanotubes (IsoSol-S100, Raymor Industries Inc.) were used in this study. Polydimethylsiloxane (PDMS) was purchased from Ellsworth Adhesives. Certified ACS grade acetone, toluene, and sodium hydroxide were purchased from Fisher Scientific. 1 mg/mL Δ9-tetrahydrocannabinol in methanol and 25 mg/mL Δ9-tetrahydrocannabinol in ethanol was purchased from Sigma Aldrich and diluted in 200 proof ethanol from Decon Laboratories for use in the bubbler. Fast Blue B Salt (dye content ~95%) was purchased from Sigma Aldrich.

2. Chemiresistor Fabrication

The 2x2 mm silicon dies with 4 pairs of interdigitated gold electrodes (IDE) was fabricated using standard photolithography processes (Figure 1a). The silicon dies were then wirebonded and potted into standard 40-pin ceramic dual in-line packages using polydimethylsiloxane (PDMS) to secure the die and the wirebonds. Semiconductor enriched singled-walled carbon nanotubes (IsoSol S-100, Raymor Industries, Inc.) were deposited as thin films on the interdigitated gold electrodes using dielectrophoresis (DEP) using a Keithley 3390 Arbitrary Waveform Generator. 5 µL of 10 µg/mL IsoSol solution was dropped on top of the silicon die and a sine wave (10 V_{pp}, 100 kHz, 2 min) was applied between the IDEs. The chemiresistors were rinsed with toluene, acetone, and water then annealed in an oven at 120°C to dry off any bound solvent molecules.

3. Carbon Nanotube Spectroscopic Characterization

3.1 Raman Spectroscopy

Horiba Scientific XploRA/SmartSPM confocal TERS system was used to obtain the Raman spectra of the nanotubes deposited on the silicon chip. A 638 nm (24mW) wavelength laser was used at 10% power.

Acquisition time of 1 sec with 10 accumulations was used to acquire the spectra. A 300 μm hole and a 100 μm slit were used with the 100x objective.

3.1 UV-Vis-NIR Spectroscopy

5 μL of P2 SWCNT and IsoSol-S100 solutions (10 μg/mL) were drop-cast on a 1 cm by 1 cm quartz slide and dried on a hotplate set to 150°C. The drop-cast process was repeated 10 times so that a visible layer of SWCNT film formed on the quartz slides. The UV-Vis-NIR spectra of the nanotube deposited quartz slides were acquired PerkinElmer Lambda 900 spectrophotometer (200 to 2600 nm).

4. THC/Ethanol Bubbler Calibration

The bubbler (Figure 1b) was assembled using a 250 mL Duran glass bottle, Duran GL 45 connection system caps and accessories, and 1.5 mm ID PTFE tubing purchased from Sigma Aldrich. The inlet tubing of the bubbler was connected to Bronkhorst EL-FLOW Prestige mass flow controller (MFC), which delivered Ultra Zero Grade dry air from gas cylinders supplied by Matheson Tri-Gas at a flow rate of 500 sccm. The bubbler was filled with ethanol dissolved THC analytical standard (0.1 mg/mL). The outlet tubing was placed directly on a whole or approximately 0.6 mm diameter hole punched pieces Whatman 150 mm diameter filter paper.

4.1 UV-Vis Absorption Spectra based Calibration

Vapor generated from the bubbler was captured on a hole punched out filter paper in a 2 dram glass vial and exposed to cumulative durations of 4.5, 9.5, 19.5, 49.5, 109.5, 229.5, or 469.5 minutes. To extract out the THC, 100 μL of ethanol was added to the vial and incubated at room temperature over-night and then placed in the freezer until the time of UV-Vis absorption measurement (250 to 350 nm). A linear calibration plot of a known concentration of THC/ethanol solution was generated by taking the absorbance at 276 nm (Figure 1c). The absorbance at 276 nm for the THC vapor extract (Figure S4a) was then used to calculate the approximate THC vapor generated by the bubbler assuming 100% capture and retention of the THC vapor (Figure S4b).

4.2 Fast Blue B Dye Colorimetric based Calibration

Vapors generated from the bubbler was captured on the filter paper for 1, 2, 4, and 8 hours (Figure S4c). Vapor generated from a bubbler containing only ethanol was also captured for 8 hours as a negative control. The outline of the tubing was marked with a pencil to keep track of the vapor exposed areas. The solution or vapor exposed areas on the filter paper were then developed with drops of Fast Blue B dye solution (2.5 mg/mL in 0.1 M NaOH), which yields red to violet color in the presence of THC molecules. Images of the filter paper were taken approximately 2 hours after the dye solution exposure when all the water had evaporated (Figure S4c).

To determine the approximate concentration of the captured THC vapor, a series of THC dissolved ethanol solutions (0.2 μL) with known THC concentrations were deposited on to a filter paper (Figure S4c). The outer edge of the wetted spot was marked with a pencil after the solution stopped spreading, which yielded a spot size approximately 1cm. When reacted with the Fast Blue B dye, a noticeable color gradient was observed going from red to pink to white associated with high to low THC concentration. The limit of detection for the Fast Blue B dye test is likely between approximately 10 ng per mm^2, which was calculated by dividing the known mass of deposited THC by the approximate spot size.

5. Sensing Experiment

Conductivity of the chemiresistor was measured using Keithley SMU 2602B SourceMeter by sourcing 5 V and measuring the current every second. A Keithley 3706A System Switch was used to switch among the 4 devices at a rate of 0.1 seconds. The Keithley equipment and MFC were synchronized and programmed using LabView 2016 software. Five seconds before the vapor exposure, the voltage from the source meter unit (SMU) was dropped to 0 V and then brought back up to 5 V, 30 seconds after the bubbler was turned off.

6. Breathalyzer Prototype

6.1 Electronics

The prototype comprised of an Arduino Uno with on-board Atmel Microcontroller Unit (MCU), a Monochrome LCD screen (i.e., with accompanying I2C programmable daughter board), a pushbutton switch, a rocker switch, a 9-V Battery, a potentiometer, and ZIF-connector, used to mount the 40-pin DIP-packaged chemiresistor. The LCD Screen, rocker switch, push-button switch, and potentiometer are panel-mounted. Please see the following section, "Plastic Enclosure," detailing the 3D printed case for details on the case assembly. Additionally, the Arduino's USB Type-B Jack is accessible through the case. The electronics and the required connections are shown in Figure 3d.

6.2 Software/Usage

Arduino software was written in the Arduino IDE. The software control diagram is shown in Figure S1. A summary of the software design and control are as follows. Upon Power-on (i.e., toggling the panel-mount rocker switch), the software enters the MCU initialization sequence to configure program memory (i.e., loading variables, establishing event handling sequences, etc.), followed by displaying a user prompt on the LCD to begin the pre-measurement calibration process. The user is directed to turn the panel-mount potentiometer knob (i.e., "Turn Counter") until the LCD display's "ADC" field reads "ADC=512". The user has 5 minutes to complete the pre-measurement calibration process. The user must wait until the 5-minute timer expires, after which, the user is directed to initiate a measurement by applying a sample through the plastic mouthpiece located at the enclosure's side.

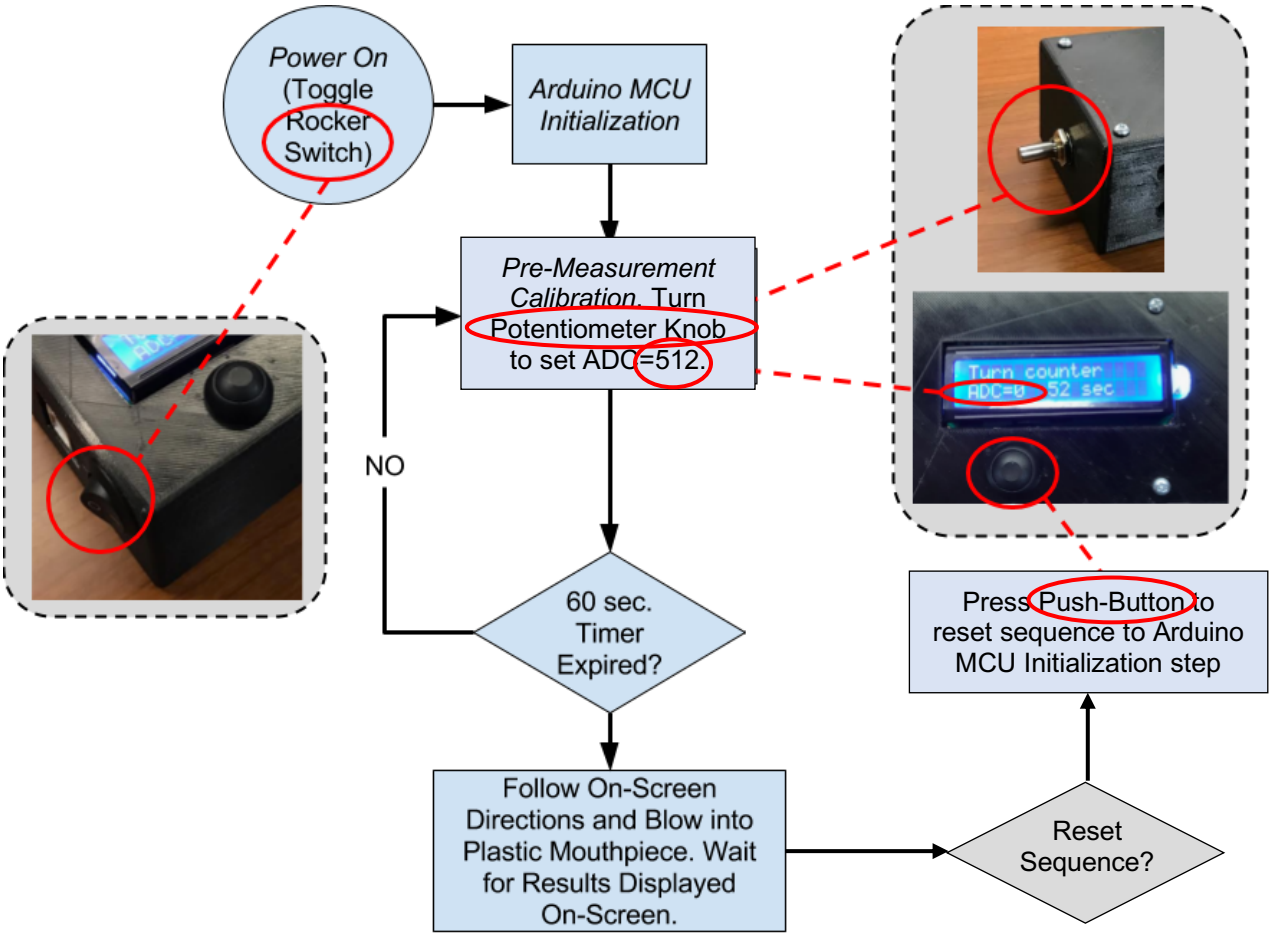

Figure S1. Prototype software and usage sequence diagram.

6.3 Plastic Enclosure

Prototype #1's enclosure was designed in the 3D CAD Modeler SolidWorks. The SolidWorks model was 3D printed on an Ultimaker printer using copolyester (CPE) Filament. The designed model and 3D printed case are shown in Figure S2. For structural integrity reasons required during the 3D printing procedure, panel-mount holes are drilled into the case after 3D printing. The enclosure's mounting holes used heat-set threaded brass inserts.

a

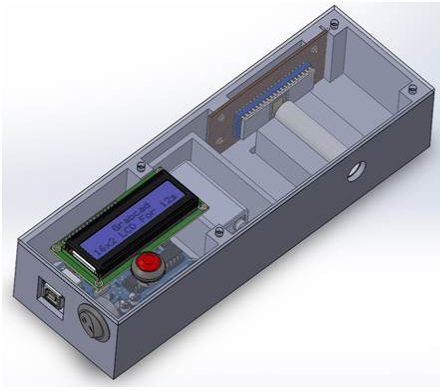

b

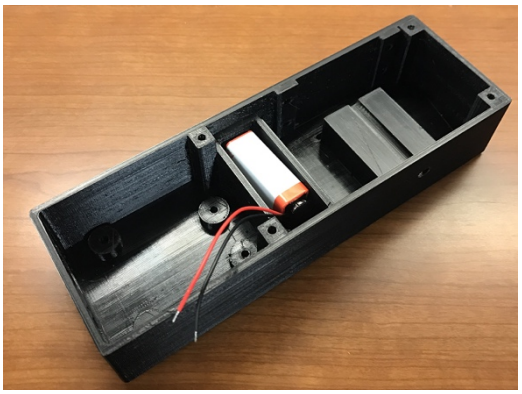

Figure S2. Prototype enclosure. (a) Rendered image of the prototype enclosure with assembled parts. (b) Image of the 3D printed enclosure with 9 V battery inside for size reference.

6.4 Assembly

The prototype electronics were installed according to Figure 3b. Electrical connections and routing were accomplished using 12” insulated multi-strand wire with rectangular housing contact female terminations. The wires are cut to length, soldered, and heat-shrink tubing applied at wire-solder connection points. The ZIF-connector for mating the 40-pin DIP-packaged CNT sensors was fastened to a small section of Perfboard. The Perfboard was then mounted to the enclosure.

A 3/8” 4-40 fully-threaded zinc-plated steel round-head screw sanded to length passes through the enclosure top lids then mates to the brass inserts. Screw lengths varied from one part of the design to another, because of unknown depth requirements.

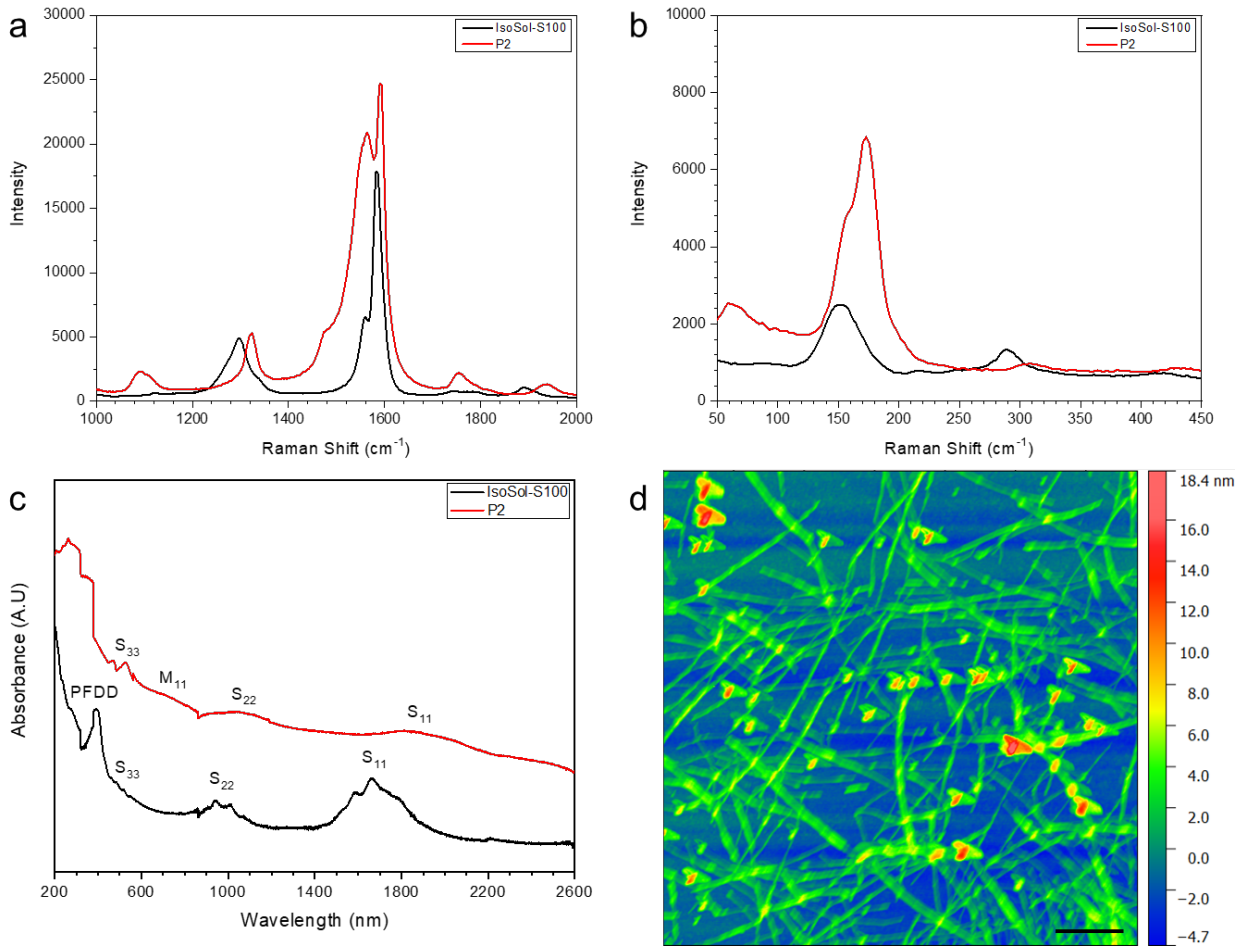

Figure S3. SWCNT characterization. (a) Raman spectra of the D and G bands. (b) Raman spectra of the radial breathing mode. (c) UV-Vis-NIR spectra of IsoSol-S100 s-SWCNT deposited on a quartz slide. (d) AFM micrograph of IsoSol-S100 on a silicon die (scale bar = 500 nm).

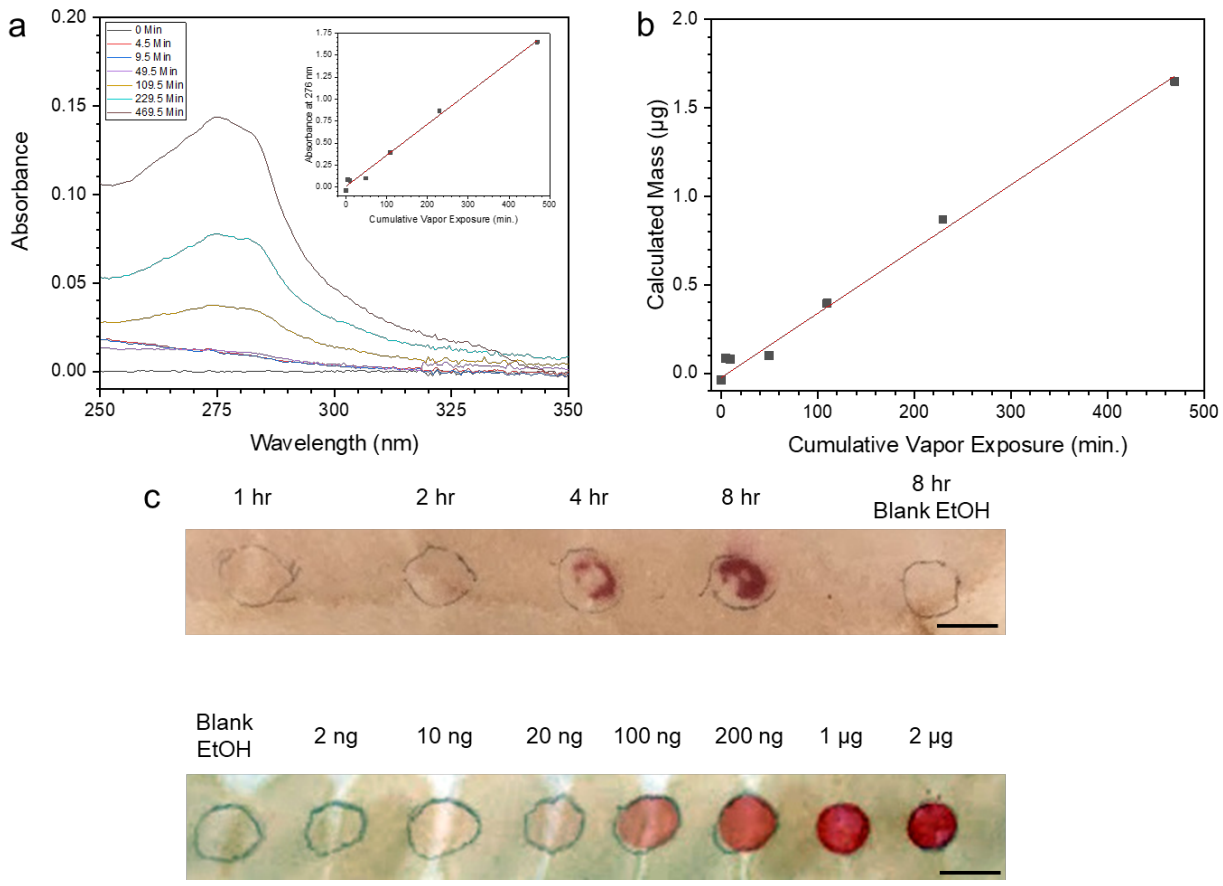

Figure S4. THC bubbler calibration. (a) UV-Vis absorption spectra of THC/ethanol standards of known concentration. (b) Calibration plot generated from the absorbance at 276 nm. (c) Top Row: THC vapor generated from the bubbler captured on a filter paper. Bottom Row: 0.1 µL of THC standards applied to the filter paper. Both rows were exposed to the Fast Blue B solution. Scale bar = 1 cm.

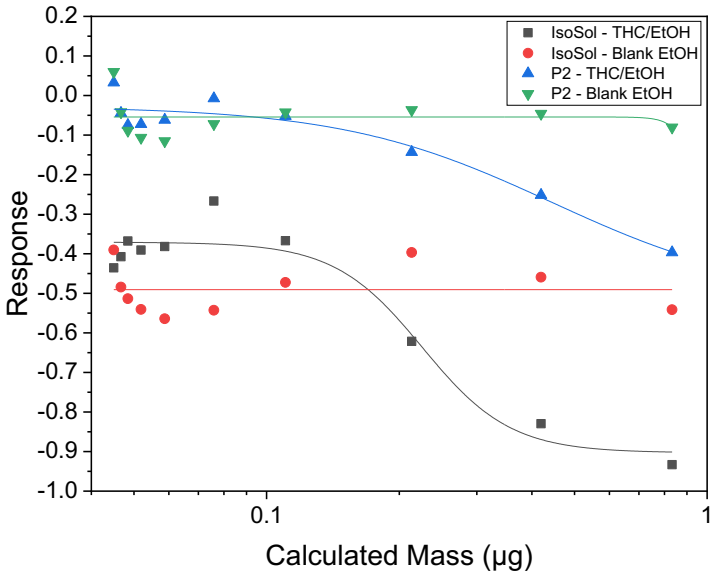

Figure S5. Relative response calibration. A calibration plot calculated using Eq. 1.

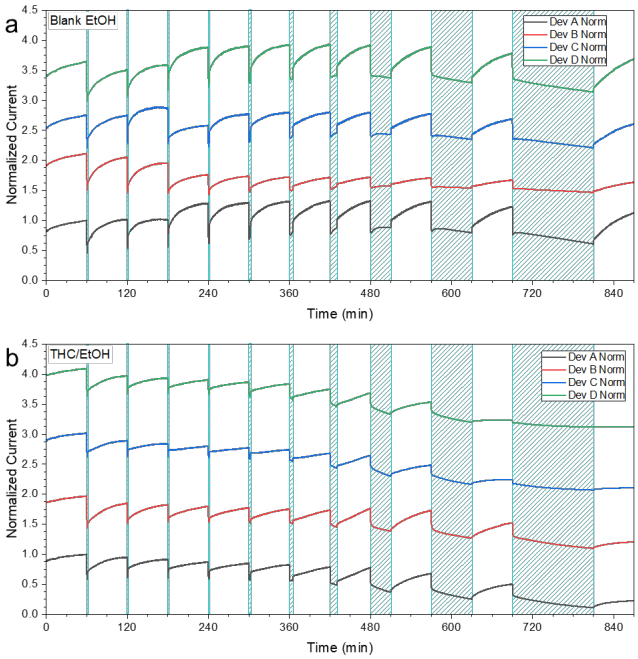

Figure S6. Blank ethanol and THC/ethanol sensing with IsoSol S-100 at constant 50 mV. If the sensor bias is held constant and not released during vapor exposure, there is a tendency for the conductivity to change inconsistently as seen at the 180-minute mark for the blank ethanol (a). Two of the devices increase in conductivity, while the other two decrease in conductivity. The inconsistency makes it difficult to distinguish between ethanol (a) and THC (b).

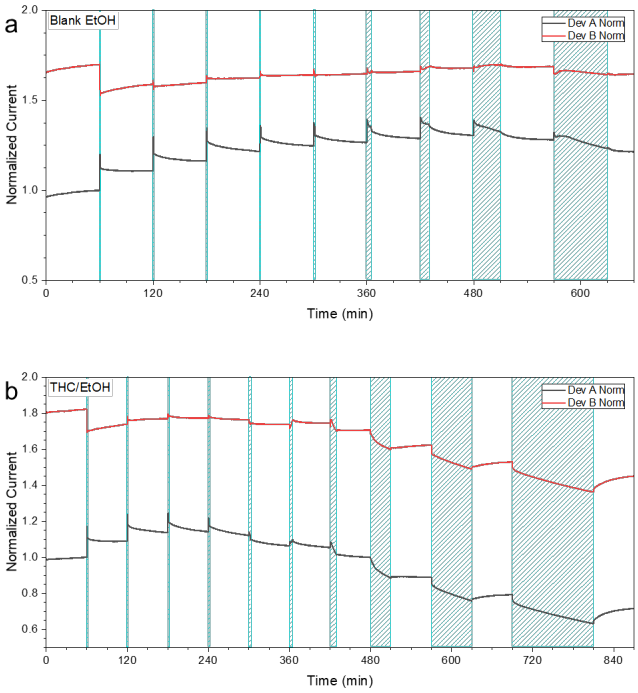

Figure S7. Blank ethanol and THC/ethanol sensing with P2 at constant 50 mV. If the sensor bias is held constant and not released during vapor exposure, there is a tendency for the conductivity to change inconsistently as seen at the 180-minute mark for the blank ethanol (a). Two of the devices increase in conductivity, while the other two decrease in conductivity. The inconsistency makes it difficult to distinguish between ethanol (a) and THC (b).

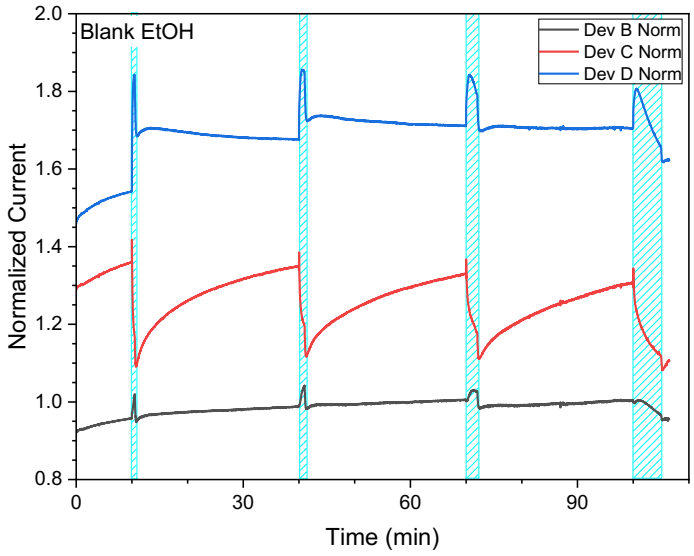

Figure S8. THC/ethanol sensing with IsoSol S-100 at constant 5 V. When the conductivity of the IsoSol chemiresistor is measured at 5 V, which corresponds to the voltage output from the Arduino prototype board, the spikes in conductivity during vapor exposure more pronounced.

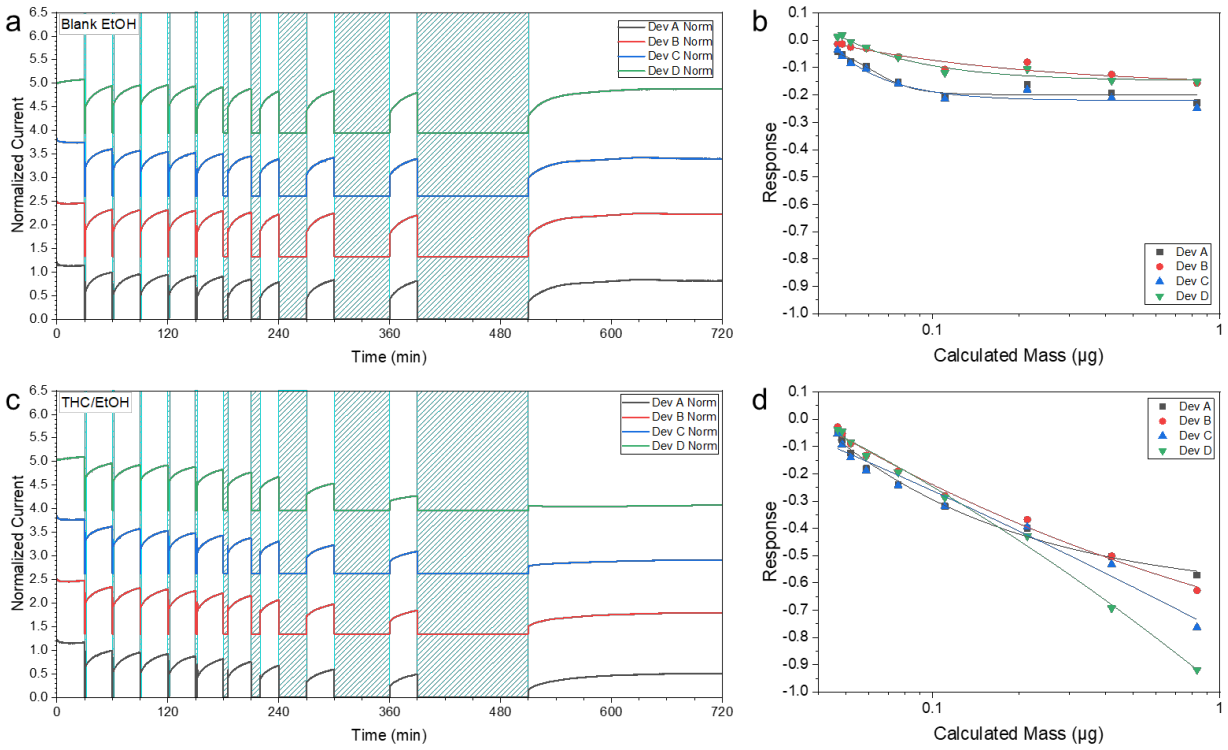

Figure S9. Blank ethanol and THC/ethanol sensing with IsoSol S-100 at On/Off 5 V. If the bias of the chemiresistor is turned off during ethanol (a) and THC/ethanol (c) vapor exposure, the conductivity of the devices does not spike unpredictably but more consistently in response to the presence of ethanol and THC vapor. (b) Calibration of the devices exposed to blank ethanol. (d) Calibration of the devices exposed to THC/ethanol.

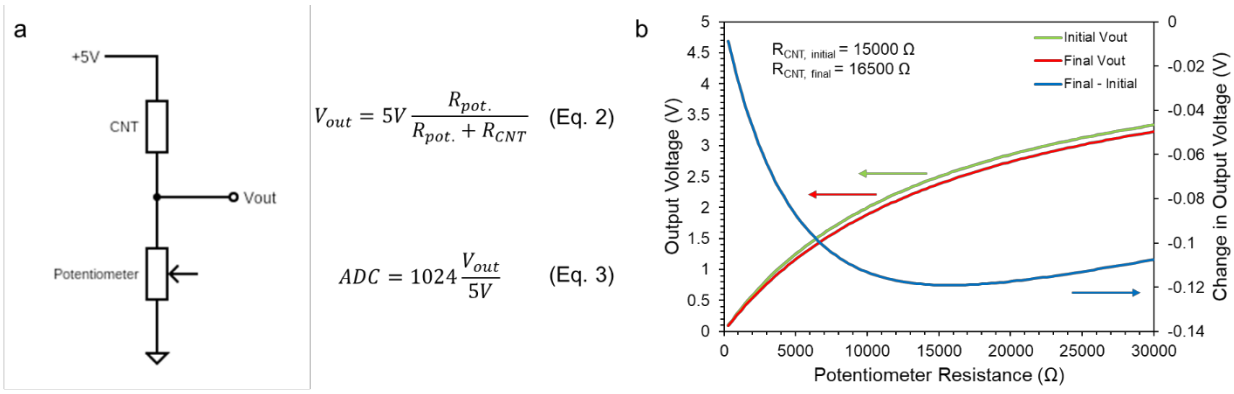

$$V_{out} = 5V\frac{R_{pot.}}{R_{pot.} + R_{CNT}} \quad \text{(Eq. 2)}$$

$$ADC = 1024\frac{V_{out}}{5V} \quad \text{(Eq. 3)}$$

Figure S10. Chemiresistor and a reference potentiometer in a voltage divider configuration. (a) The THC chemiresistor and a reference potentiometer is connected in series to form a voltage divider. The output voltage between the reference potentiometer and the chemiresistor follows equation 2 and is measured by the Arduino board. The 10-bit Analog-to-Digital Converter (ADC) in the Arduino Uno board then converts the analog into a 10-bit number (1-1024) following equation 3. (b) The maximum change in the output voltage (blue) in the voltage divider for a 10% increase in chemiresistor resistance, which is the approximate resistance increase for the 20x THC/ethanol vapor exposure, is observed when the chemiresistor resistance and potentiometer resistance are approximately equal in value. The recommended zeroing of ADC in the prototype Pre-measurement Calibration Step (Figure S1) is to maximize the signal even for the smallest change in sensor resistance.